ALEKSANDER LEICHT, KRZYSZTOF MAKOWSKI*

# THE EMPLOYMENT OF A SINGLE-PHASE CAPACITOR INDUCTION MOTOR FOR STAND-ALONE GENERATING OPERATION

## ZASTOSOWANIE JEDNOFAZOWEGO SILNIKA INDUKCYJNEGO Z POMOCNICZYM UZWOJENIEM KONDENSATOROWYM DO AUTONOMICZNEJ PRACY GENERATOROWEJ

Abstract

The paper presents a two-dimensional field-circuit model of a two-winding, single-phase induction machine operating as single-phase, self-excited induction generator. The model takes remnant magnetism and magnetization characteristics of the stator and rotor core into account. Results of simulations and experiments are presented, i.e. waveforms of voltages during self-excitation, their dependence on rotor slot opening, influence of capacitances and different capacitor topologies on self-excitation, as well steady-state values of generator voltages and currents at no-load operating conditions. Terminal voltage and currents in stator windings as a function of rotor speed and capacitances of capacitors for resistive loads are also presented. The possibility of directly supplying a single-phase induction motor from the generator as a dynamic load were also investigated. Obtained simulation and experimental results show the need for use of semi-closed rotor slots to ensure conditions for successful self-excitation. The obtained simulation results were validated experimentally on the laboratory setup.

*Keywords*: *induction generator*, *single-phase*, *self-excitation*, *field-circuit modeling*

Streszczenie

W artykule przedstawiono dwuwymiarowy model polowo-obwodowy dwuuzwojeniowej, jednofazowej maszyny indukcyjnej pracującej jako samowzbudny generator indukcyjny. Model ten uwzględnia (w sposób uproszczony) istnienie remanentu magnetycznego w rdzeniu maszyny oraz charakterystyki magnesowania blach pakietów stojana i wirnika. Zaprezentowane zostały wyniki badań symulacyjnych oraz eksperymentalnych – przebiegi napięć podczas procesu samowzbudzenia generatora w zależności od szerokości otwarcia żłobków wirnika, z uwzględnieniem wpływu pojemności i układów kondensatorów w uzwojeniach generatora na przebieg procesu samowzbudzenia oraz na wartości ustalone napięć i prądów w stanie jałowym. Przedstawiono także zmiany napięcia na zaciskach generatora i w uzwojeniu wzbudzenia oraz prądów stojana w zależności od prędkości obrotowej generatora oraz zastosowanych pojemności i układów kondensatorów w uzwojeniach stojana przy obciążeniu rezystancyjnym i przy zasilaniu jednofazowego silnika indukcyjnego. Uzyskane wyniki symulacji i pomiarów wskazują na konieczność zastosowania w wirniku jednofazowego samowzbudnego generatora indukcyjnego żłobków półzamkniętych w celu zapewnienia warunków do zainicjowania procesu samowzbudzenia. Otrzymane na drodze symulacji charakterystyki zostały pozytywnie zweryfikowane na stanowisku laboratoryjnym.

*Słowa kluczowe*: *generator indukcyjny*, *jednofazowy*, *samowzbudzenie*, *modelowanie polowo-obwodowe*

* M.Sc. Eng. Aleksander Leicht, D.Sc. Ph.D. Eng. Krzysztof Makowski, prof. of WrUT, Department of Electrical Engineering, Chair of Electrical Machines, Drives and Measurements, Wroclaw University of Technology, Poland.

## 1. Introduction

Single-phase, self-excited induction generators (SPSEIG), driven by internal combustion engines, small wind or hydro turbines can be used as an additional or reserve source of electrical energy in households or in remote areas. Induction generators are characterized by their simple construction (i.e. brushes and permanent magnets are not used), and their low cost of manufacturing, maintenance and ruggedness when compared with synchronous and DC generators. Considerate interest in induction generators was observed, since renewable energy sources became a viable alternative to conventional sources [1–8]. Most of the available works deal with three-phase SEIG, while a two-winding, single-phase induction machine may also be successfully utilized [1, 2, 5]. The single-phase induction machine may operate as a self-excited induction generator, when its main and auxiliary windings are electrically separated and an excitation capacitor is connected to its auxiliary (excitation) winding. The main winding becomes a load winding, to which the load is connected. In the majority of available papers, steady-state and transient analysis is done with the help of a classical circuit model – equivalent circuit for steady state and *dq* model for transients [1, 3, 5]. Classical models are convenient, however, lumped parameter based analysis greatly simplify the phenomena associated with varying magnetic flux in the machine's core, e.g. self-excitation, skin effect or saturation. The use of a two-dimensional field circuit model, based on the finite element method, allows for precise determination of parameters and transient and steady-state characteristics, taking into account the phenomena associated with the varying magnetic field [11]. Design and analysis of SEIG, which operates when the magnetic core is saturated, may be effectively performed by using a field-circuit model [8, 9]. For the first time, this model was applied to the single-phase self-excited induction generator in [6, 7], where the residual magnetism was modeled as a weak permanent magnet embedded in the rotor core.

The paper presents the examination of performance of the single-phase self-excited induction generator by simulation and experiments with both no-load and load conditions.

## 2. Field-circuit model of the generator

The physical support for the study is represented by a two-phase induction machine, designed for motor operation, characterized by the main data – rated power of 1.1 kW, rated voltage of 230 V, 4 poles. The physical symmetry and electromagnetic periodicity allows for the reduction of the two-dimensional computation domain to half of the cross-section (two pole pitches) of the machine, as shown in Fig. 1. The finite element mesh includes about 20 thousand second-order triangular and quadrangular elements. The computation domain is delimited by the outer surface of the stator core and inner surface of the rotor core. Zero magnetic flux boundary conditions are applied to those surfaces.

The stator windings of the generator are unsymmetrical, the single-layer, two-phase copper windings: main winding (marked by $M$ in Fig. 1) is the output winding of the generator, and the load is connected to its terminals, while the auxiliary winding ($A$ in Fig. 1) operates as the excitation winding with excitation capacitor connected to its terminals. The aluminum rotor cage consists of 30 bars, placed in semi-closed slots, the width of the slot opening $b_r$ = 1 mm.
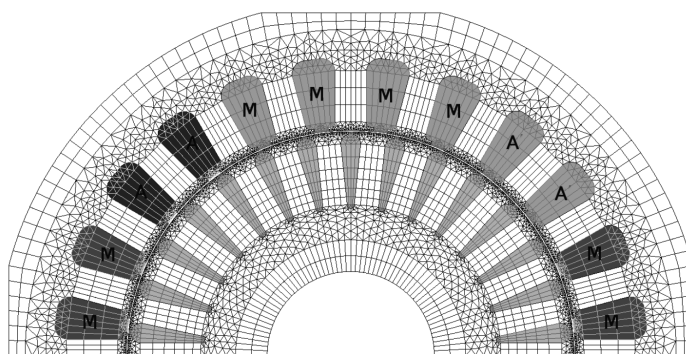
Fig. 1. Two-dimensional field model of the SPSEIG

An electrical circuit associated with the field model is depicted in Fig. 2 – this consists of the following components:
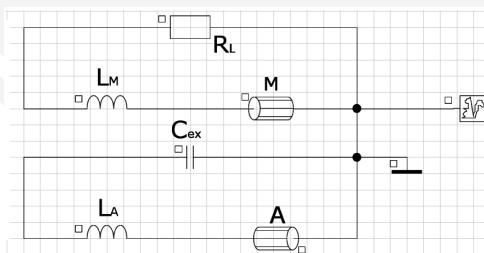


Fig. 2. Circuit part of the field-circuit model of the SPSEIG

- *M* and *A* are respective phases of the winding; these components are direct couplings between circuit and field parts of the model,
- $L_M$ and $L_A$ are leakage inductances of stator winding end connections,
- $C_{ex}$ is the excitation capacitor,
- $R_L$ is the load resistance,
- The squirrel symbol in Fig. 2 represents a macro-circuit used to model the cage rotor, consisting of rotor bars (field-circuit couplings), along with resistances and leakage reactances of the inter-bar section of short-circuit rings (circuit components).

The magnetic field in different parts of the generator's cross-section may be described by the following equations:

$$curl\left(v \cdot curl\mathbf{A}\right) = \begin{cases} \mathbf{J_S} & \text{in stator winding} \\ \mathbf{J_S} - \sigma \cdot \partial\mathbf{A}/\partial t & \text{in rotor bars} \\ 0 & \text{in airgap and magnetic core} \end{cases} \tag{1}$$

where:
$A[0,0,A(x,y,t)]$ – the magnetic vector potential,
$J_s[0,0,J_s(x,y,t)]$ – the current density in the stator slots,
$v$　　　　　 – the magnetic reluctivity of the core,
$\sigma$　　　　　 – the electric conductivity.

Field computations were performed with the non-linear magnetization characteristics of the stator and rotor core taken into account.

The simulation results have been validated using the laboratory set-up, which comprises the SPSEIG, driven by a three-phase motor fed by frequency inverter. A view of the tested machine as a main part of the laboratory set-up is shown in Fig. 3.
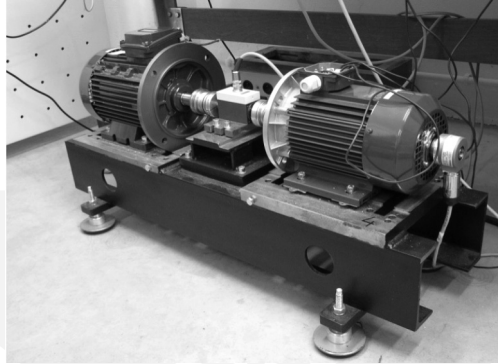


Fig. 3. Laboratory set-up for experimental study of the SPSEIG

## 3. Self-excitation of single-phase induction generator

### 3.1. Modeling of residual magnetism

Contemporary available FEM software programs, including Cedrat Flux2D, do not allow taking magnetic hysteresis into account, therefore, three approximate methods of modeling the remnant flux density were applied:

1. Placing the source of magnetic flux (non-zero boundary condition) on the inner diameter of rotor core
2. Placing a thin layer of current in the airgap
3. Initiating the magnetic flux as a result of current flowing in the auxiliary winding while the excitation capacitor discharges.

The values of magnetic flux, current density and initial capacitor voltage in respective methods have been chosen to obtain terminal voltages corresponding to remnant voltage measured in the experiments. Simulation results of self-excitation for each method for a topology with two capacitors ($C_{sh}$ = 15 µF, $C_{ex}$ =30 µF) are shown in Fig. 4. For each method, the steady-state voltage is close to the rated voltage, however, the time needed for voltage build-up is different for every method. The third method was employed for further study, as time of voltage build-up for this is closest to the experimental results (Fig. 4d)).

An influence of the rotor slot opening and its width on self-excitation process is illustrated in Fig. 5. For the wider slot opening the longer is the build-up time of the stator voltage. Width of rotor slot opening does not significantly affect the RMS value of the terminal voltage.
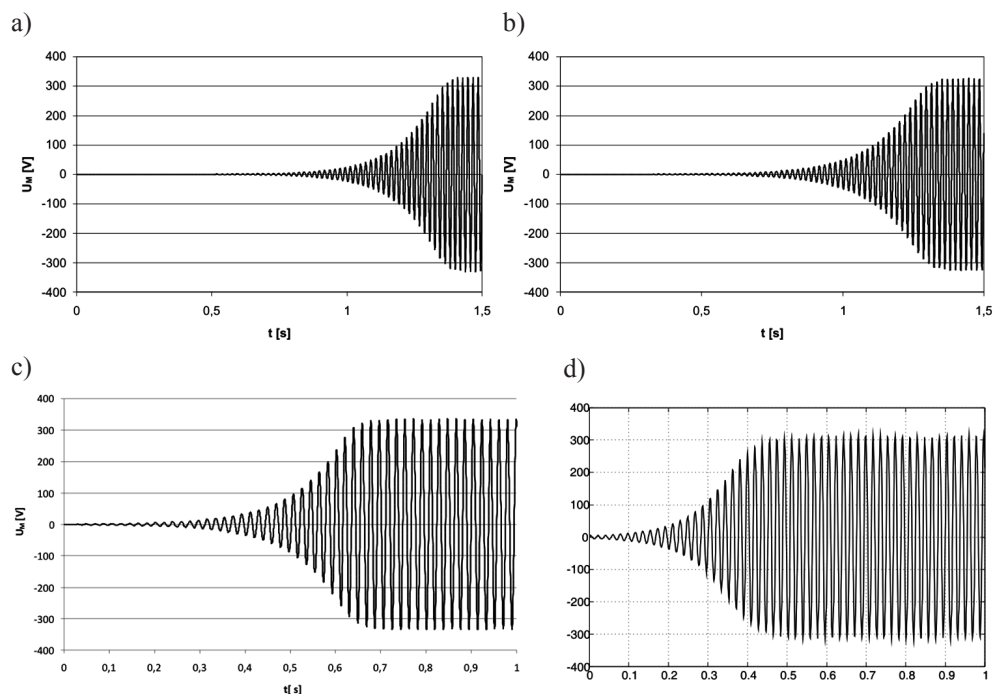
a)



b)

c)

d)

Fig. 4. Main winding voltage during self excitation: residual magnetism modeled by: a) the 1st method; b) 2nd method; c) 3rd method; d) measurement

## 3.2. Significance of rotor slot opening for self-excitation process
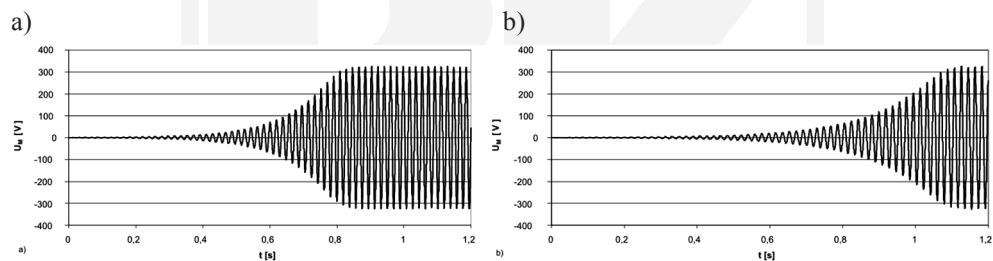
a)

b)

Fig. 5. Main winding voltage waveform during self-excitation: a) $b_r = 0.5$ mm; b) $b_r = 2$ mm

In small power induction motors, closed rotor slots are often used to reduce noise, torque pulsations and starting current due to large leakage rotor reactance. When closed rotor slots are used in induction generator, voltage build-up may not take place, because the magnetic flux induced by the stator currents passes through bridges above the rotor slots, as shown in Fig. 6a), and does not induce currents in the rotor bars. The resultant magnetic flux does not increase and the voltage in the stator windings die out, i.e. the voltage build-up does not take place. Figure 7 shows experimental results for the machine with closed rotor slots. The pre-charged excitation capacitor is switched at the instant of time 0.1 s. The induced low voltage

visible at the beginning of the waveform is the result of residual flux density in the rotor core. The capacitor discharges after being switched on, and self-excitation does not occur – the voltages settles at a level dependent upon the remnant flux.
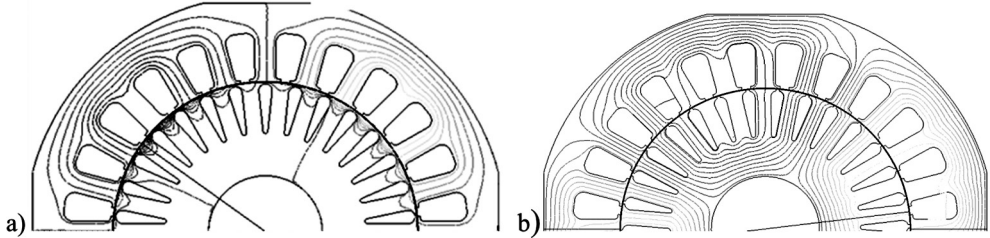


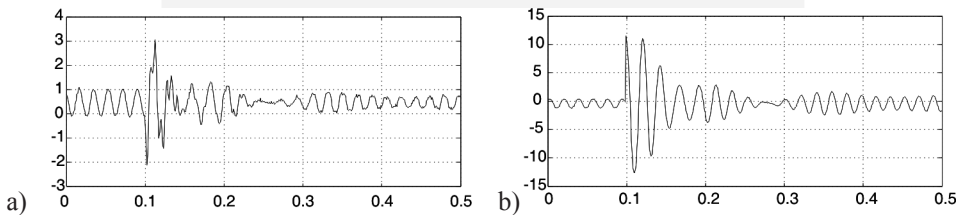Fig. 6. Magnetic flux lines in SPSEIG: a) closed rotor slots; b) semi-closed rotor slots



Fig. 7. Voltage waveforms during unsuccessful voltage build-up – experimental results:
a) main winding voltage; b) auxiliary winding voltage

## 4. Influence of capacitor's capacitances and prime mover speed on no-load voltages and currents

Figures 8a)–c) show the dependence of no-load voltages in the main and auxiliary windings and auxiliary winding current on the prime mover rotational speed and excitation capacitance $C_{ex}$ for capacitor topology with excitation capacitor only, as shown in Fig. 8d). As might be expected, terminal voltage $U_M$ is strongly dependent on the rotor speed and capacitance $C_{ex}$, and it is not possible to obtain a voltage close to the rated value (230 V), even for large capacitances and speeds far exceeding the synchronous speed of the machine as the magnetic core is deeply saturated. Limits of speed and capacity below which self-excitation will not take place can be read from Fig. 8, i.e. $C_{ex}$ = 30 µF for $n$ = 1380 rpm and $C_{ex}$ = 25 µF for $n$ = 1380–1560 rpm. It should be noted that auxiliary winding voltage $U_A$ reaches levels exceeding the rated value.

Applying shunt capacitor to the main stator winding (Fig. 9e)) improves operating conditions by the more efficient exploit of both the windings and the iron core. Simulation and experimental results for the topology with excitation and shunt capacitors are shown in Fig. 9 ($C_{ex}$ = 30 µF). This solution allows obtaining rated terminal voltage. It is seen that the shunt capacitance $C_{sh}$ has no major effect on the main winding current $I_M$ of the generator and it is possible to control terminal voltage by modulation of the shunt capacitance.
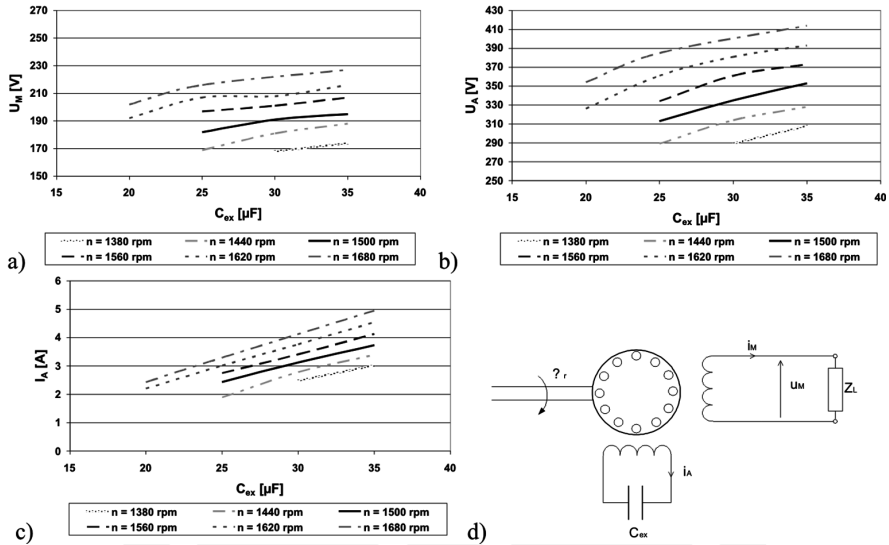
Fig. 8. No-load characteristics of the generator for different values of $C_{ex}$ and rotor speed, for the topology with excitation capacitor only: a) main winding voltage $U_M$; b) auxiliary winding voltage $U_A$; c) auxiliary winding current $I_A$; d) connection scheme
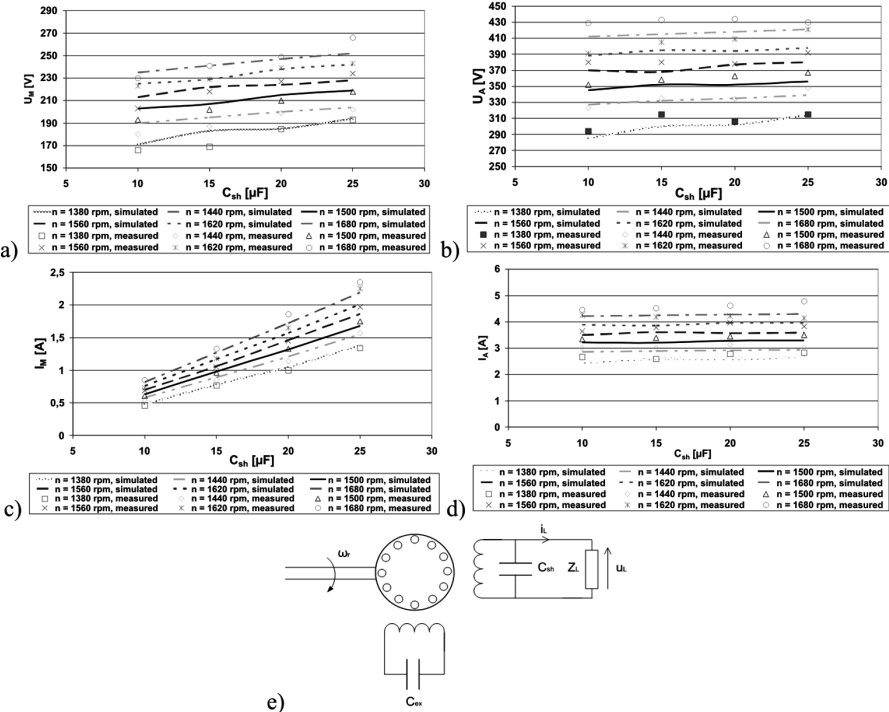


Fig. 9. No-load characteristics of the generator for different values of $C_{sh}$ and rotor speed, for the shunt capacitor topology: a) main winding voltage $U_M$; b) auxiliary winding voltage $U_A$; c) main winding current $I_M$; d) auxiliary winding current $I_A$; e) capacitor connection scheme

## 5. Load characteristics of SPSEIG

Simulation and experimental results presented in Fig. 10 show that the SPSEIG with the shunt capacitor in the main winding may operate stably with a resistive load up to approximately 50% of the machine's rated power, while with the resistant-inductive load, the range of stable operation decreases with decreasing the power of the factor of the load (Fig. 10c)).
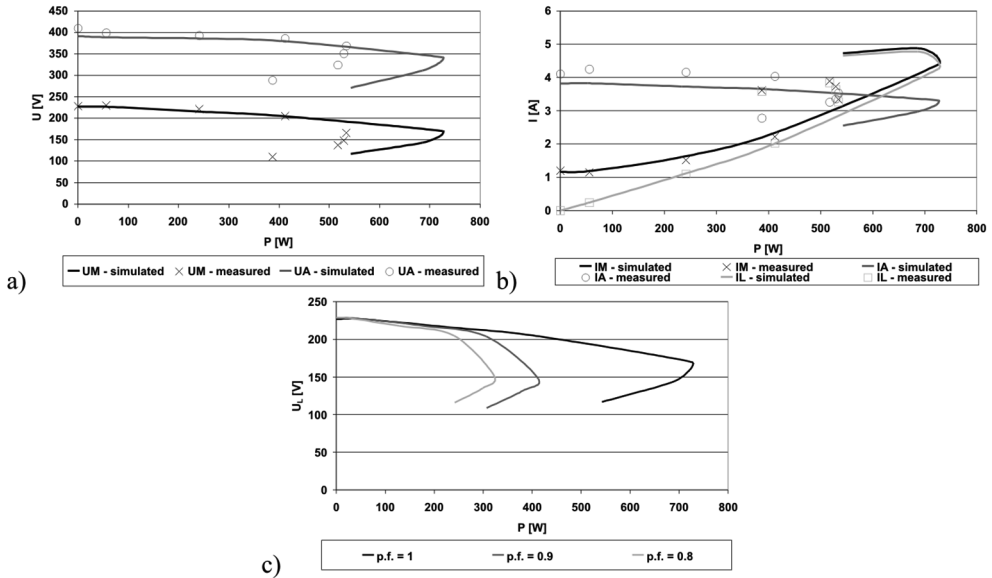


Fig. 10. Voltages and currents versus output power of the SPSEIG with shunt capacitor topology: a) main ($U_M$) and auxiliary ($U_A$) winding voltage for resistive load; b) main winding ($I_M$), auxiliary winding ($I_A$), and load current ($I_L$) for resistive load; c) terminal voltage for different power factors

Load range of the SPSEIG may be easily extended by applying the short-shunt capacitor topology (Fig. 11) – the generator may be loaded up to the rated power when the load is purely resistive. For the resistant-inductive load output power of the generator, as in the previous case, decreases after power factor decreasing.

Figure 12 shows voltage and current waveforms of the SPSEIG with shunt topology measured during switching of the dynamic load – the single-phase capacitor induction motor of rated power $P_n = 90$ W. During motor start-up, a terminal voltage drop and current increase may be noticed, as the induction motor intakes reactive power from the generator. If the SPSEIG is to supply induction motors, e.g. small pumps, special attention should be paid, because too large a starting current may demagnetize the generator leading to terminal voltage collapse. Simple remedial measures, like a damping resistor, may be used to limit the starting current of the induction motor.
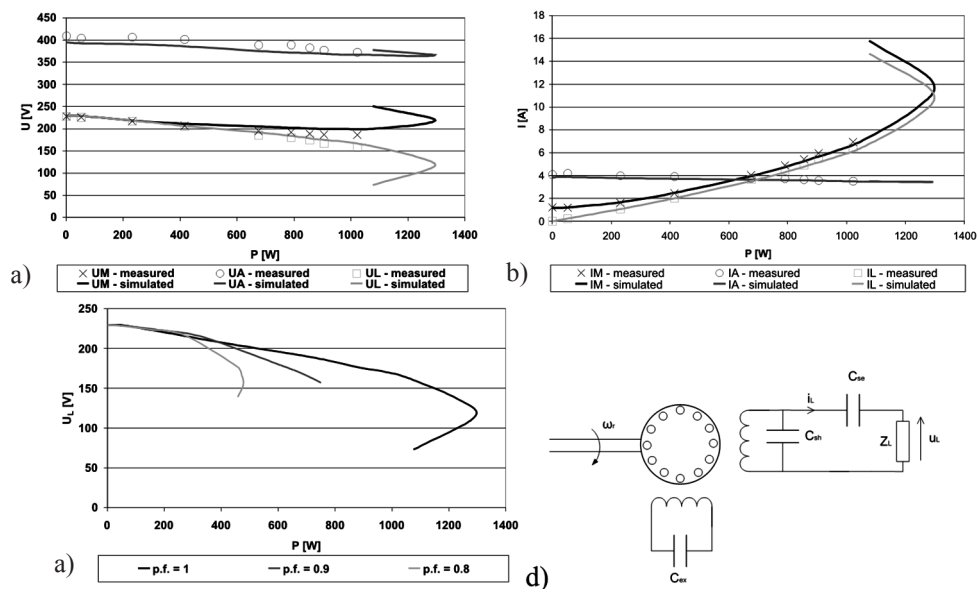
Fig. 11. Voltages and currents versus output power of the SPSEIG with short-shunt capacitor topology: a) main ($U_M$) and auxiliary ($U_A$) winding voltage for resistive load; b) main winding ($I_M$), auxiliary winding ($I_A$), and load current ($I_L$) for resistive load; c) terminal voltage for different power factors; d) capacitor connection scheme
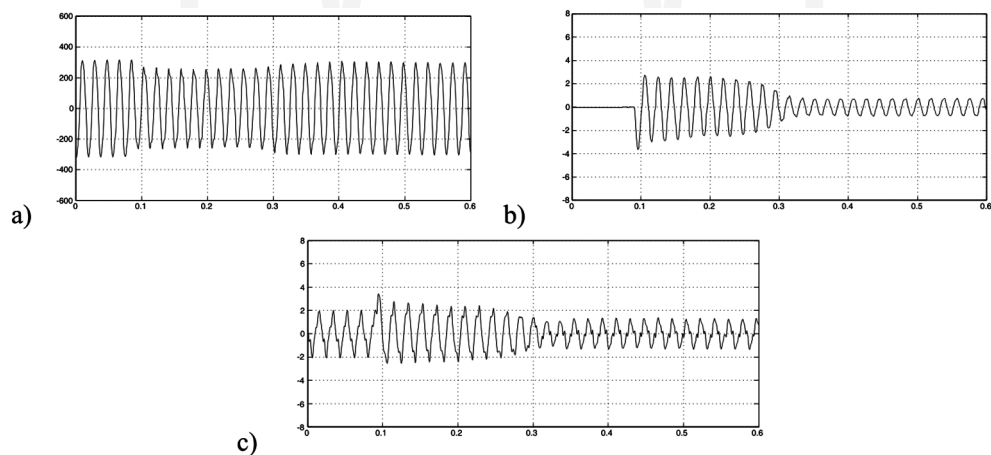


Fig. 12. Measured voltage and current waveforms of the generator before and after switching of an induction motor: a) terminal voltage, b) load current, c) main winding current

## 6. Conclusions

In the paper, the FEM-based, field-circuit model of single-phase, self-excited induction generator was presented. An investigation of the single-phase induction machine designed as the induction motor in respect to possible employment as an autonomous self-excited induction generator was presented. Analysis of the influence of the rotor slot opening showed that semi-closed rotor slots should be used to ensure self-excitation of the generator by remnant magnetic flux in the rotor left from previous operation events. In the case of closed rotor slots of the tested machine, the relatively weak remnant flux density does not induce currents in the rotor cage, so the self-excitation process can not be initiated. The detailed study shows that, for a resistive load, the short-shunt capacitor topology provides stable operation conditions up to the rated power of the machine. The possibility of directly supplying the single-phase capacitor induction motor from the generator as a dynamic resistant-inductive load was also presented. The simulation results obtained by the field-circuit model of the generator were successfully verified by laboratory tests.

References

[1] Murthy S.S., Singh B., Sandeep V., *A Novel and Comprehensive Performance Analysis of a Single-Phase Two-Winding Self-Excited Induction Generator*, IEEE Transactions on Energy Conversion, March 2012, Vol. 27, No. 1, pp. 117–127.
[2] Leicht A., Makowski K., *Self-excitation analysis of a single-phase induction generator*, XVI International Symposium on Electromagnetic Fields in Mechatronics, Electrical and Electronic Engineering, ISEF, Ohrid, Macedonia, Sept. 12–14, 2013.
[3] Makowski K., Leicht A., *Analysis of operation of a single-phase self-excited induction generator by a field-circuit model*, XVI International Symposium on Electromagnetic Fields in Mechatronics, Electrical and Electronic Engineering, Ohrid, Macedonia, Sept. 12–14, 2013.
[4] Leicht A., Makowski K., A *single-phase induction motor operating as a self-excited induction generator*, Archives of Electrical Engineering, 2013, Vol. 62(3), pp. 361–373.
[5] Ojo O., Omozusi O., Jimoh A.A., *The operation of an inverter-assisted single-phase induction generator*, IEEE Transactions on Industrial Electronics, Jun 2000, Vol. 47, No. 3, pp. 632–640.
[6] Rajanathan C.B., Edward A.J.G., Hu G., *Finite element study of a single phase induction generator*, Sixth International Conference on Electrical Machines and Drives, 1993, Conf. Publ. No. 376, pp. 252–257.
[7] Rajanathan C.B., Watson B.J., *Simulation of a single phase induction motor operating in the motoring, generating and braking modes*, IEEE Transactions on Magnetics, May 1996, Vol. 32, No. 3, pp. 1541–1544.
[8] Tudorache T., Melcescu L., Paturca S.V., *Finite Element Analysis of Self-Excited Induction Generator for Isolated Small Power Wind Turbines*, International Conference on Clean Electrical Power, ICCEP '07, 21–23 May, 2007, pp. 656–661.

[9] Sawetsakulanond B., Kinnares V., *Design, analysis, and construction of a small scale self-excited induction generator for a wind energy application*, Energy, December 2010, Vol. 35, Issue 12, pp. 4975–4985, ISSN 0360-5442.

[10] Björnstedt J., Sulla F., Samuelsson O., *Experimental investigation on steady-state and transient performance of a self-excited induction generator*, Generation, Transmission & Distribution, December 2011, IET, Vol. 5, No. 12, pp. 1233–1239.

[11] Kumbhar G.B., Kulkarni S.V., Escarela-Perez R., Campero-Littlewood E., *Applications of coupled field formulations to electrical machinery*, COMPEL, 2007, Vol. 26, Issue 2, pp. 489–523.